Recent results on kaonic atoms from theory

Jaroslava Óbertová

Faculty of Nuclear Sciences and Physical Engineering,
Czech Technical University in Prague

in collaboration with

Àngels Ramos — University of Barcelona

Eliahu Friedman — *Hebrew University, Jerusalem*

Jiří Mareš — *NPI, Řež*

Workshop on Fundamental Physics with Exotic atoms,
23 - 25 June 2025, Frascati, Italy

K^-N interaction

- K^-N interaction near threshold described by chiral coupled-channel interaction models

  A. Cieply, J. Smejkal, NPA 881 (2012) 115 - Prague (P)

  Y. Ikeda, T. Hyodo, W. Weise, NPA 881 (2012) 98 - Kyoto-Munich (KM)

  A. Feijoo, V. Magas, A. Ramos, PRC 99 (2019) 035211 - Barcelona (BCN)

  Z. H. Guo, J. A. Oller, PRC 87 (2013) 035202 - Murcia (M1 and M2)

  M. Mai, U.-G. Meißner, NPA 900 (2013) 51 - Bonn (B2 and B4)

- Model parameters fitted to K^-p scattering data, treshold branching rations and shift and width of kaonic hydrogen

Kaonic atoms

- Info about $K^- N$ interaction below threshold provided by kaonic atoms

  65 data points (energy shifts, widths, yields=upper level widths) from CERN, Argonne, RAL, BNL

- Chirally motivated models fail to describe kaonic atom data

  E. Friedman, A. Gal, NPA 959 (2017) 66

model	B2	B4	M1	M2	P	KM
$\chi^2(65)$	1174	2358	2544	3548	2300	1806

Multinucleon processes

- Chiral models include only $K^- N \to \pi Y$ ($Y = \Lambda, \Sigma$) decay channel
- K^- interactions with two and more nucleons should be included, (e.g., $K^- + N + N \to Y + N$) $\leftarrow$ analysis of kaonic atom data
  E. Friedman, A. Gal, NPA 959 (2017) 66

$$V^{\mathrm{phen}}_{K^-\mathrm{multiN}} = -4\pi B(\frac{\rho}{\rho_0})^{\alpha}\rho$$

B is a complex amplitude, ρ is nuclear density distribution, ρ_0 is saturation density and α is positive

- equally good description of data with $\chi^2/\mathrm{dof} \leq 2$

Single- vs. multi-nucleon processes

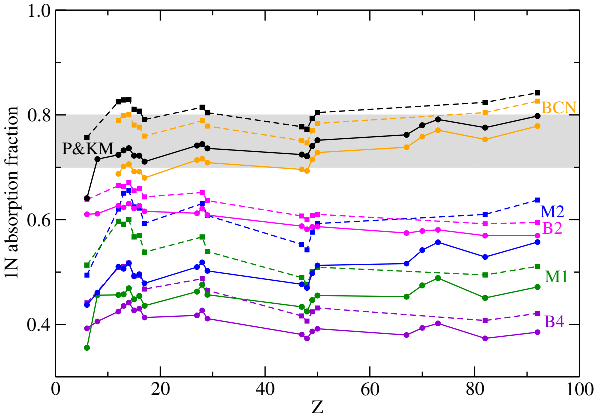

- Fraction of *single-nucleon* absorption 0.75 ± 0.05 (average value) used as an additional constraint.

→ Only P, KM and BCN models found acceptable in kaonic atom analysis

E. Friedman, A. Gal, NPA 959 (2017) 66

AMADEUS@DAΦNE

K. Piscicchia et al., PLB 782 (2018) 339

$$|f^{s}_{ar}| = (0.334 \pm 0.018\,\mathrm{stat}^{+0.034}_{-0.058}\mathrm{syst})\ \mathrm{fm}\,.$$

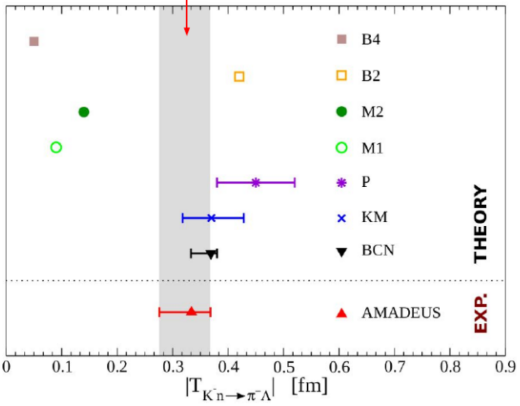

K. Piscicchia, talk at THEIA-STRONG2020 Web-Seminar,20 December 2020

Multinucleon processes

- K^- multi-nucleon absorption in the surface region of atomic nuclei represents about 20%

  NC 53 (1968) 313 (Berkeley), *NPB 35 (1971) 332 (BNL)*, *NC 39A (1977) 538 (CERN)*

- K^- multi-nucleon absorption in atoms described by phenomenological optical potential

  E. Friedman, A. Gal, NPA 959 (2017) 66

- Model for K^-NN absorption in nuclear matter using free-space chiral amplitudes

  T. Sekihara et al., PRC 86 (2012) 065205

- New experimental data on K^-NN absorption (AMADEUS@DAΦNE)

  K. Piscicchia et al., PLB 782 (2018) 339

  R. Del Grande et al., EPJ C79 (2019) 190

- Solid microscopic model for K^-NN absorption needed!

Microscopic model for $K^- NN$ absorption in nuclear matter

Microscopic model for K^- two-nucleon absorption in symmetric nuclear matter *J. Hrtánková, À. Ramos, PRC 101 (2020) 035204*

- based on a meson-exchange approach
  H. Nagahiro et al., PLB 709 (2012) 87
- P and BCN chiral $K^- N$ amplitudes employed
- Pauli correlations in the medium for $K^- N$ amplitudes considered
- real part of the $K^- NN$ optical potential evaluated as well
- $K^- N$ optical potential derived within the same approach

$K^- N$ absorption in nuclear matter

$$K^- N \to \pi Y \quad (Y = \Lambda, \Sigma)$$

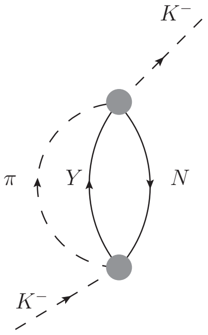

Fig.1: Feynman diagram for K^- absorption on a single nucleon in nuclear matter. The shaded circles denote the $K^- N$ t-matrices derived from a chiral model.

K^-NN absorption in nuclear matter

$$K^- + N + N \to Y + N \quad (Y = \Lambda, \Sigma)$$

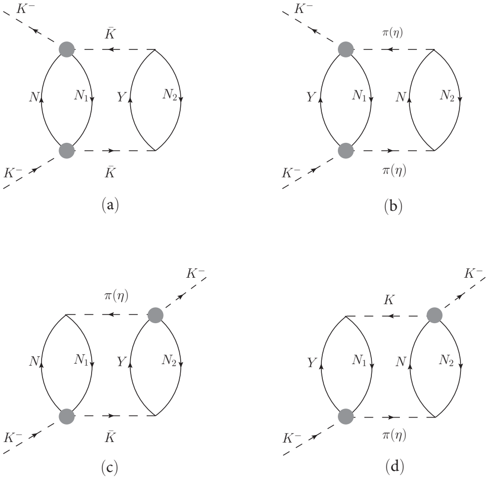

Fig.2: Two-fermion-loop (2FL) Feynman diagrams for non-mesonic K^- absorption on two nucleons N_1, N_2 in nuclear matter. The shaded circles denote the K^-N t-matrices derived from a chiral model.

K^-NN absorption in nuclear matter

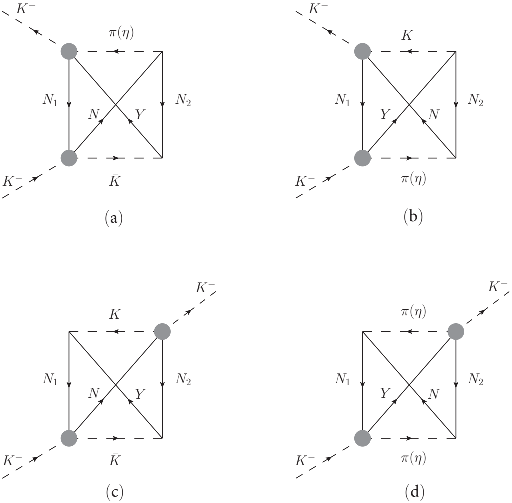

Fig.3: One-fermion-loop (1FL) Feynman diagrams for non-mesonic K^- absorption on two nucleons N_1, N_2 in nuclear matter. The shaded circles denote the K^-N t-matrices derived from a chiral model.

$K^{-}NN$ absorption in nuclear matter

$V_{K^-N} = \sum_{channels} V_{K^-N \to \pi Y}$ (Fig.1)

$V_{K^-NN} = \sum_{\mathrm{channels}} V^{\mathrm{2FL}}_{K^-NN} + V^{\mathrm{1FL}}_{K^-NN}$ (Fig.2 and 3)

$\to$ contributions from 37 2FL and 28+33 1FL diagrams

Table 1: All considered channels for mesonic and non-mesonic K^- absorption in matter.

K^-N	$\to \pi Y$	$K^-N_1N_2$	$\to YN$
K^-p	$\to \pi^0\Lambda$	K^-pp	$\to \Lambda p$
	$\to \pi^0\Sigma^0$		$\to \Sigma^0 p$
	$\to \pi^+\Sigma^-$		$\to \Sigma^+ n$
	$\to \pi^-\Sigma^+$	$K^-pn(np)$	$\to \Lambda n$
K^-n	$\to \pi^-\Lambda$		$\to \Sigma^0 n$
	$\to \pi^-\Sigma^0$		$\to \Sigma^- p$
	$\to \pi^0\Sigma^-$	K^-nn	$\to \Sigma^- n$

AMADEUS: Ratio for 2N absorption

Recently measured ratio *R. Del Grande et al., EPJ C79 (2019) 190*

$$R = \frac{\mathrm{BR}(K^- pp \to \Lambda p)}{\mathrm{BR}(K^- pp \to \Sigma^0 p)} = 0.7 \pm 0.2(\mathrm{stat.})^{+0.2}_{-0.3}(\mathrm{syst.})$$

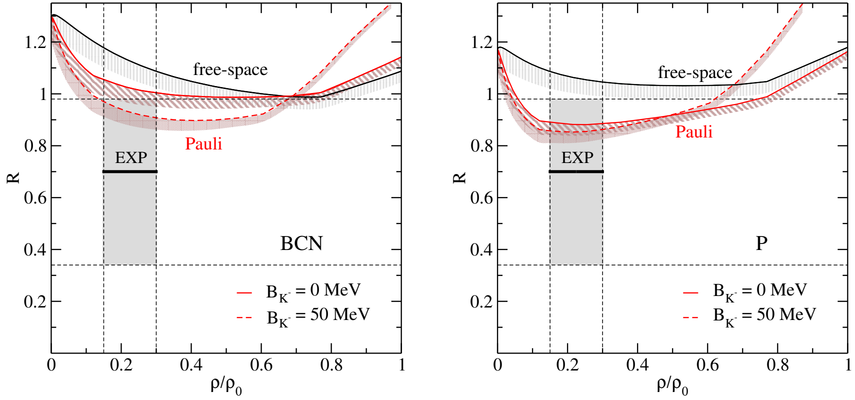

Fig.4: The ratio R as a function of relative density, calculated using the free-space and Pauli blocked amplitudes for $B_{K^-} = 0$ MeV and $B_{K^-} = 50$ MeV. Color bands denote the uncertainty due to different cut-off values $\Lambda_c = 800 - 1200$ MeV.

The role of hadron self-energies

- inclusion of Y, N, K^- and π self-energies into the K^-N chiral BCN amplitudes as well as into the K^-NN model.
- considered baryon potentials

$$V_N = -70\frac{\rho}{\rho_0}\ \mathrm{MeV},$$

$$V_\Lambda = -58\frac{\rho}{\rho_0} + 31\left(\frac{\rho}{\rho_0}\right)^2 \rightarrow V_\Lambda(\rho_0) = -26.4\ \mathrm{MeV},$$

$$V_\Sigma = 30\frac{\rho}{\rho_0}\ \mathrm{MeV}.$$

- considered pion S- and P-wave self-energy

  A. Ramos, E. Oset, NPA 671 (2000) 481

The role of hadron self-energies: $K^- p$ amplitudes

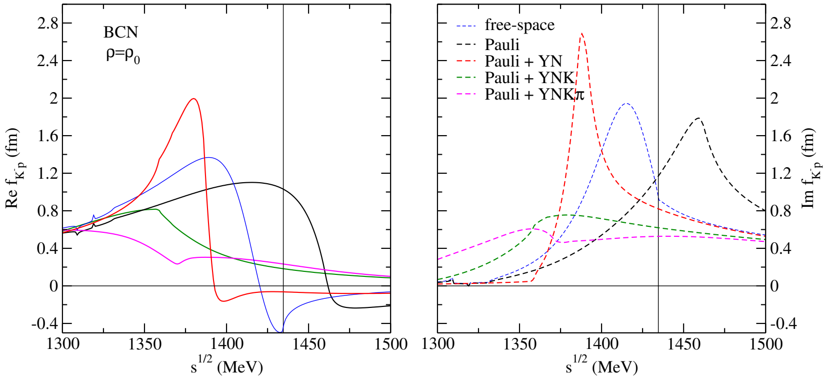

Fig.5: Comparison of $K^- p \to K^- p$ BCN amplitudes with Pauli blocking only (black), Pauli+YN SE (red), Pauli + YNK^- SE (green), and Pauli + $YNK^-\pi$ SE (magenta) at saturation density $\rho_0 = 0.17$ fm^{-3}.

The role of hadron self-energies: $K^- n$ amplitudes

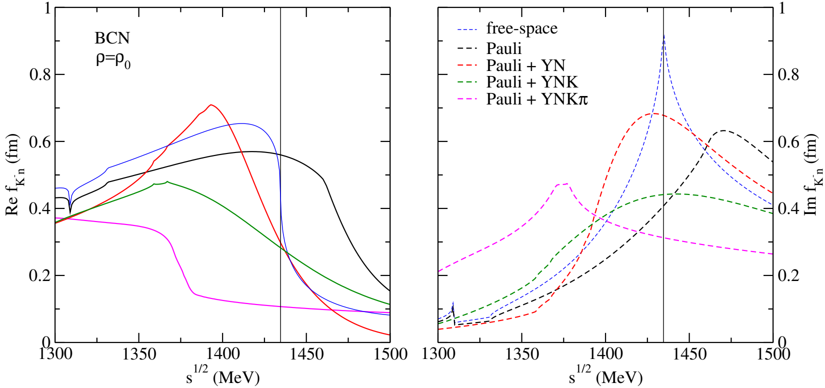

Fig.6: Comparison of $K^- n \to K^- n$ BCN amplitudes with Pauli blocking only (black), Pauli+YN SE (red), Pauli + YNK^- SE (green), and Pauli + $YNK^-\pi$ SE (magenta) at saturation density $\rho_0 = 0.17$ fm^{-3}.

Comparison with AMADEUS measurement

K. Piscicchia et al., PLB 782 (2018) 339

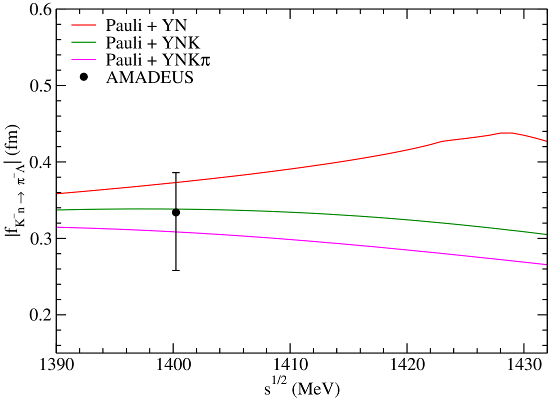

Fig.7: Comparison of $|f_{K-n\to\pi-\Lambda}|$ measured by AMADEUS with in-medium amplitudes: Pauli + YN SE (red), Pauli+YNK SE (green), and Pauli + $YNK^-\pi$ SE (magenta) from the BCN model (taken at $\rho = 0.3\rho_0$).

The role of hadron self-energies: K^- potential

- Pauli + YN SE amplitudes $\Rightarrow V_{K^-} = V_{K^-N} + V_{K^-NN}$
- Pauli + $YNK^-(YNK^-\pi)$ SE amplitudes

$$\Downarrow$$

$$V_{K^-} = t\rho + V^{\mathrm{corr}}_{K^-NN}$$

$$\swarrow \qquad \searrow$$

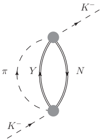

+

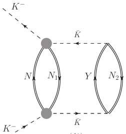

(d1)

+ ... +

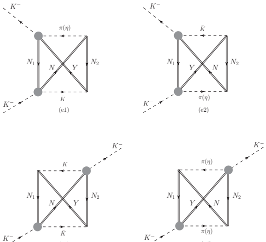

(e1) (e2) (e3) (e4)

The role of hadron self-energies: K^- potential

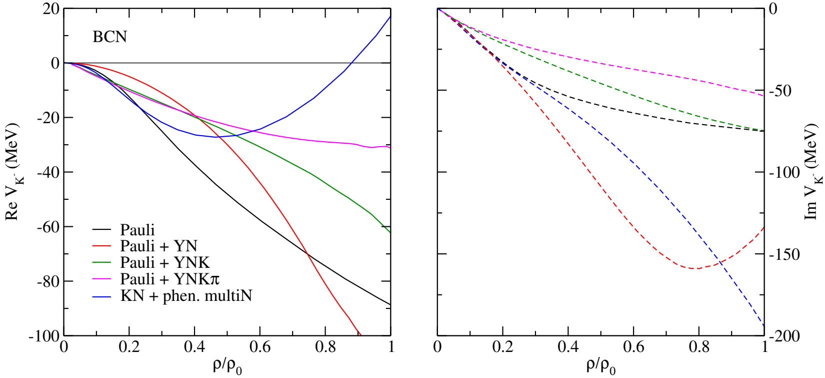

Fig.8: Real (left) and imaginary (right) parts of the total K^- potential as a function of relative density ρ/ρ_0, calculated with Pauli (black), Pauli + YN SE (red), Pauli + YNK^- SE (green), and Pauli + $YNK^-\pi$ SE (magenta) BCN amplitudes. For comparison there is the best fit K^-N + phen. multiN potential (blue) based on BCN amplitudes.

Calculations of kaonic atoms

Table 3: Values of $\chi^2(65)$ obtained in calculations of kaonic atoms (24 nuclear species, 65 data points) using $K^-N + K^-NN$ potentials based on BCN Pauli, Pauli+YN, Pauli+YNK, and Pauli+YNKπ amplitudes. For comparison, there are also results of calculations with K^-N+phen. multiN potential based on WRW modified BCN amplitudes *(T. Wass, M. Rho, W. Weise, NPA 617 (1997) 449)*.

BCN	Pauli	Pauli+YN	Pauli+YNK	Pauli+YNKπ	WRW
	$K^-N + K^-NN$	$K^-N + K^-NN$	$t\rho + V^{corr}_{K^-NN}$	$t\rho + V^{corr}_{K^-NN}$	K^-N + phen. multiN
$\chi^2(65)$	553.2	265.5	162.2	93.2	110.7
χ^2/dof	8.5	4.1	2.5	1.4	1.7

- A. Baca et al. *(NPA 673 (2000))* obtained value of $\chi^2/dof = 3.8$ with K^- potential based on chiral model of Oset and Ramos *(NPA 671 (2000))*.

Total K^- potential: version 2025 vs. 2000

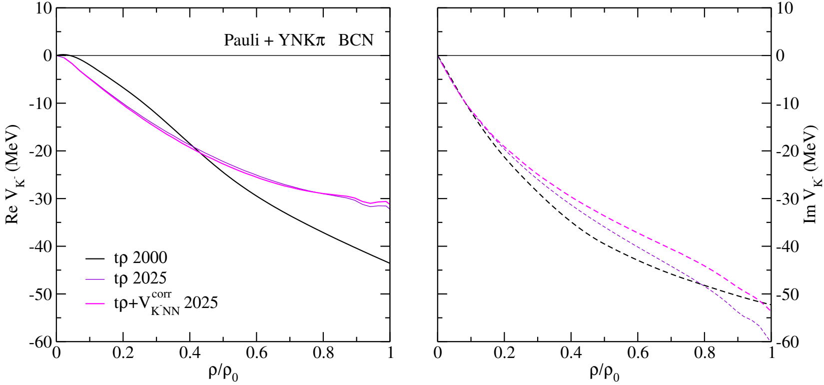

Fig.9: Real (left) and imaginary (right) parts of the total K^- potential calculated with Pauli + YNKπ (magenta) BCN amplitudes compared with the K^- optical potential including hadron SE based on the model of Oset and Ramos (black). Thin violet lines represent the $t\rho$ part of the current K^- optical potential obtained with Pauli YNKπ BCN amplitudes.

Branching ratios in ^{12}C+K^- atom

Table 4: Primary-interaction branching ratios (in %) for mesonic ($K^- N \rightarrow Y\pi$, $Y = \Lambda, \Sigma$) and non-mesonic absorption ($K^- NN \rightarrow YN$) of K^- in ^{12}C+K^- atom (3d level), calculated with total K^- potential based on Pauli + YNKπ BCN amplitudes. The experimental data corrected for primary interaction are shown for comparison.

^{12}C + K^- (3d)	BCN	Exp.	
mesonic ratio	Pauli+YNKπ	[1]	[2]
$\Sigma^+\pi^-$	14.4	29.4 ± 1.0	14.4 ± 2.3
$\Sigma^-\pi^0$	8.1	2.6 ± 0.6	1.2 ± 0.4
$\Sigma^-\pi^+$	12.8	13.1 ± 0.4	10.3 ± 1.7
$\Sigma^0\pi^-$	8.2	2.6 ± 0.6	1.2 ± 0.4
$\Sigma^0\pi^0$	10.0	20.0 ± 0.7	11.8 ± 1.4
$\Lambda\pi^0$	5.3	3.4 ± 0.2	11.8 ± 1.0
$\Lambda\pi^-$	11.1	6.8 ± 0.3	23.6 ± 1.9
total 1N ratio (3d)	70.0	77.9 ± 1.6	74.3 ± 3.9
total 1N ratio ($3d + 4f$)	71.8		
total multiN ratio (3d)	30.0	19.0 ± 2.0	25.7 ± 3.1
total multiN ratio ($3d + 4f$)	28.2	21 ± 3(stat.)$^{+5}_{-6}$(syst.) [3]	

[1] *C. Vander Velde-Wilquet et al., NC 39 A (1977) 538*

[2] *H. Davis et al., NC 53 A (1968) 313*

[3] *R. Del Grande et al., EPJ C79 (2019) 190*

Branching ratios for $\Sigma^{\pm}\pi^{\mp}$ channels from FINUDA

Table 5: Primary-interaction ratios (in %) for the $\Sigma^{-}\pi^{+}$ and $\Sigma^{+}\pi^{-}$ channels in light kaonic atoms calculated using the Pauli+YNKπ BCN amplitudes. Experimental data from the FINUDA collaboration are corrected for pion attenuation and for $\Sigma N - \Lambda N$ conversion with 50 % probability for both Σ's.

	Pauli+YNKπ		Exp. [4]	
nucleus (nl)	$\Sigma^{+}\pi^{-}$	$\Sigma^{-}\pi^{+}$	$\Sigma^{+}\pi^{-}$	$\Sigma^{-}\pi^{+}$
^{6}Li ($3d$)	16.0	20.4	36.7 $\pm$ 1.6	30.0 $\pm$ 1.1
^{7}Li ($3d$)	12.2	13.0	16.4 $\pm$ 0.5	13.4 $\pm$ 1.3
^{9}Be ($3d$)	13.1	12.6	11.7 $\pm$ 0.4	9.2 $\pm$ 0.5
^{12}C ($3d$)	14.7	13.2	20.0 $\pm$ 0.3	15.9 $\pm$ 0.2
^{13}C ($3d$)	12.7	10.3	14.9 $\pm$ 1.0	10.1 $\pm$ 0.5
^{16}O ($3d$)	14.5	11.6	15.5 $\pm$ 0.7	13.0 $\pm$ 0.5

[4] *M. Agnello et al., PLB 704 (2011) 474*

Summary

- $K^- N$ interaction described by chiral meson-baryon coupled channel interaction models
- Interactions of K^- with two and more nucleons important for realistic description of the K^--nucleus interaction
  - only P, KM, and BCN models compatible with available data
- We have developed a microscopic model for $K^- NN$ absorption in nuclear matter using amplitudes derived from the P and BCN chiral meson-baryon interaction models

  J. Hrtánková, À. Ramos, PRC 101 (2020) 035204

  - Pauli blocked amplitudes included $\rightarrow$ medium effects non-negligible
  - Calculated ratios in a good agreement with experimental data

Summary

- Further extension of the K^-NN model and K^-N BCN amplitude model $\rightarrow$ inclusion of hadron (Y, N, K^-, π) self-energies
- Considering all hadron SE $\rightarrow$ $\mathrm{Re}\, V_{K^-}(\rho_0) \sim -30$ MeV and $\mathrm{Im}\, V_{K^-}(\rho_0) \sim -50$ MeV
- Calculations of energy shifts and widths in kaonic atoms:
  - inclusion of K^-NN absorption improves the description of data considerably

    J. Óbertová, E. Friedman, J. Mareš, PRC 106 (2022) 065201
  - **full model Pauli+$YNK\pi$ SE describes the data as good as the best fit K^-N+phen. multiN potential based on BCN amplitudes!**